Hydrology Research

Hydrology Research Vol 54 No 4, 580 doi: 10.2166/nh.2023.142

The changing precipitation storm properties under future climate change

Haijie Wang[a,b], Peng Jiang[a,b,*], Rongrong Zhang[a], Jiahui Zhao[a,b], Wei Si[b], Yong Fang[c] and Nana Zhang[b]

[a] State Key Laboratory of Hydrology-Water Resources and Hydraulic Engineering, Hohai University, Nanjing 210024, China
[b] College of Hydrology and Water Resources, Hohai University, Nanjing 210024, China
[c] Shaoxing Tangpu Reservoir Co., Ltd., Shaoxing 312364, China
*Corresponding author. E-mail: peng.jiang@hhu.edu.cn

PJ, 0000-0002-8472-1221

ABSTRACT

Changes in precipitation storm characteristics especially extreme precipitation events have been frequently reported during recent years, which poses great challenges for flood controls of reservoir basins. In this study, we present a comprehensive examination on the evolution of storm properties during two distinct rainy seasons in Changtan Reservoir Basin located on the southeastern coast of China. We compare the differences in storm duration, inter-storm period, the average storm intensity, and with-in storm pattern between the Meiyu flood season (MFS) and typhoon flood season (TFS). We also explore the future projections of these storm properties based on Coupled Model Intercomparison Project 6 (CMIP6) precipitation outputs. Our results indicate that precipitation storms in TFS exhibit shorter duration and higher average storm intensity than those of MFS, the flood risk in June is mainly due to accumulative precipitation (longer duration), while in July to September, is mainly due to the storms with high intensity. The projected precipitation shows uncertainties for different emission scenarios, especially during TFS. However, the increasing trend of the average storm intensity is relatively consistent, which is supposed to bring more pressure on flood control in the study area. The results can provide a beneficial reference to water resources management.

Key words: climate change, emission scenarios, Meiyu flood season, precipitation storm properties, Typhoon flood season

HIGHLIGHTS

- The evolution of storm properties was investigated.
- Precipitation in typhoon flood season exhibits shorter duration and higher intensity than those of the Meiyu flood season.
- Flood risk in June is mainly due to accumulative precipitation in the study area.
- Flood risk from July to September is due to storms with high intensity.
- Projected precipitation shows uncertainties but a consistent increasing trend in storm intensity.

GRAPHICAL ABSTRACT

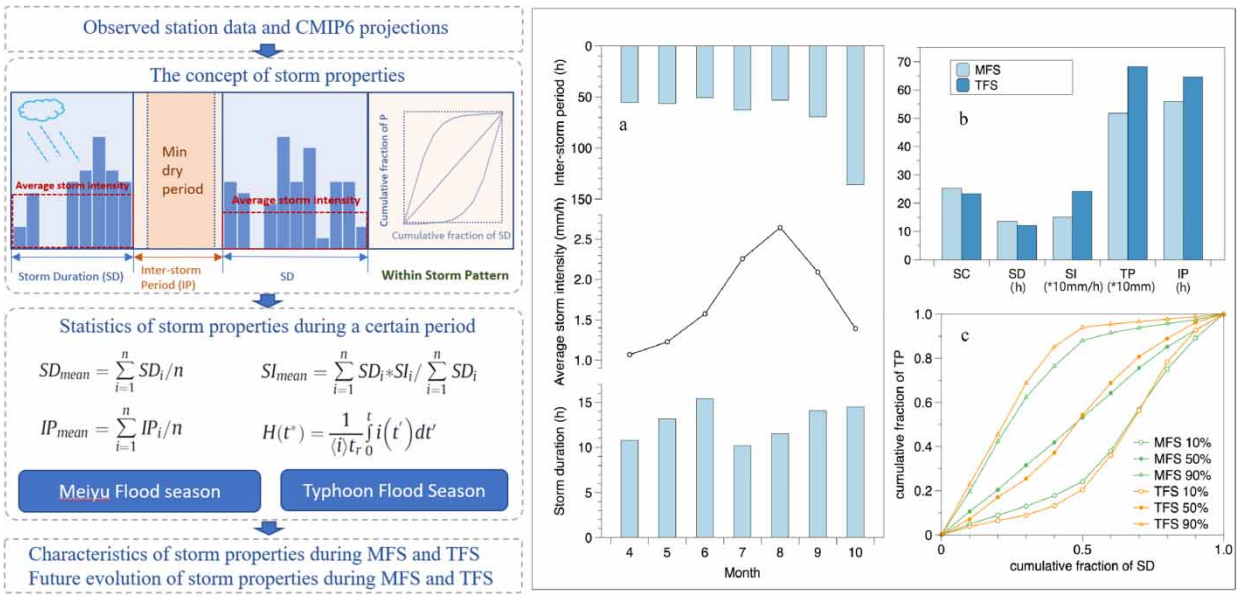

1. INTRODUCTION

Precipitation is one of the most important drivers of regional hydrological processes, yet it is also much more uncertain compared to the other climate variables such as temperature in the future projections (Chen *et al.* 2013; Wang & Chen 2014). The spatiotemporal distributions of precipitation have been altered due to changes of climate and land use (Trenberth 2011; Pathirana *et al.* 2014; Sohoulande Djebou & Singh 2016). Precipitation variations are of concern to society as the societal impacts of changes in precipitation have become more apparent. The 201.9 mm hourly rainfall in Zhengzhou, China 2021, the unusually heavy downpours in the central-western Europe, 2021, and the continuous 3 months of heavy rain in Pakistan, 2022 had profound impacts on both human society and the natural environment. Therefore, it is critical to investigate the changing pattern of precipitation in the future for flood and water resources management studies.

Precipitation variability has been examined by various methods. These methods could be broadly divided into two categories. The first one is using different precipitation indices including percentile-based indices, absolute indices representing maximum or minimum values within a certain period, threshold indices, duration indices, etc. (Jiang *et al.* 2015; Niu *et al.* 2021). Based on the definition of precipitation indices, they could be calculated for a station or a gird at a certain period and then used for the analysis of the spatiotemporal characteristics of precipitation. The second one is applying traditional intensity-duration-frequency (IDF) analysis or depth-duration-frequency (DDF) analysis (Agilan & Umamahesh 2016; Lima *et al.* 2016; Liuzzo *et al.* 2017). These methods focus more on total precipitation over a certain period rather than the concept of integrated precipitation event which has its start, development, and ending processes. The precipitation storm (referred as a storm here and after) properties are closely related to floods, soil erosion, agriculture, ecological habitat, etc. (Walther *et al.* 2002; Angel *et al.* 2005; Zhang *et al.* 2012) As a result, more analysis should be conducted on storm properties in the changing conditions.

The precipitation variations receive more attention in the southeastern coast of China as this region is undergoing rapidly changing social dynamics, pressure from an expanding population, and a greater risk of flooding (Gao *et al.* 2017; Liu *et al.* 2021). The flood season is characterized by two periods: Meiyu flood season (MFS), during which the continuous rainfall event is mainly caused by the planetary-scale Meiyu front (Ding *et al.* 2007) and Typhoon flood season (TFS) with heavy rainstorms caused by a typhoon (Tian *et al.* 2012; Gao *et al.* 2017). High intensity rainstorms during TFS may lead to severe flooding problems in this region. The intensity of rainfall during MFS is relatively small, but the large accumulation of rainfall during a long duration could also contribute to severe floods (Volonté *et al.* 2021). As the rainfall events during MFS and TFS are caused by different climatic systems, they may exhibit different trends or variations in the future. It is necessary to investigate the evolution of precipitation events separately during these two periods. Tian *et al.* (2012) investigated the trends of

extreme precipitation in both MFS and TFS and indicated that the increase in total precipitation is mainly due to the increased precipitation during TFS. However, to our knowledge, few studies are conducted to explore the precipitation variability from the perspective of storm events for MFS and TFS, and fewer studies are designed to analyze the future trends of storm properties based on the climate model outputs.

To address the knowledge gaps mentioned above, we investigate the storm properties during two flood seasons based on station precipitation records, we also explore the future trends of storm properties based on Coupled Model Inter-comparison Project 6 (CMIP6) model outputs. Mean storm duration, inter-storm period, storm intensity, and within-storm patterns are determined for both MFS and TFS in the study region, the statistical matrices of storm properties are compared to illustrate different responses of storm events to changing conditions. The thorough analyses of precipitation variability during the two flood seasons are expected to provide detailed information on precipitation evolution to forecasters and local water managers.

2. MATERIALS AND METHODS

2.1. Study area and data sources

Changtan Reservoir Basin (CRB) is selected for the analysis in this study. It is in Zhejiang Province, which belongs to the southeastern coast region of China (Figure 1). Summer is hot and rainy as it is dominated by the tropical ocean air mass, while winter is cold and dry with subtropical climate characteristics under the control of the polar continental air mass. The annual mean precipitation (1960–2021) is about 1,430 mm with two rainy periods namely Meiyu rainy season and the typhoon rainy season. The duration of the Meiyu season is usually around 20–30 days, which depends on the position and intensity of the Western Pacific Subtropical High (Qiao *et al.* 2021). Precipitation during this period exhibits a long duration and relatively lower average intensity. On the other hand, typhoon usually lands in this region from late July to

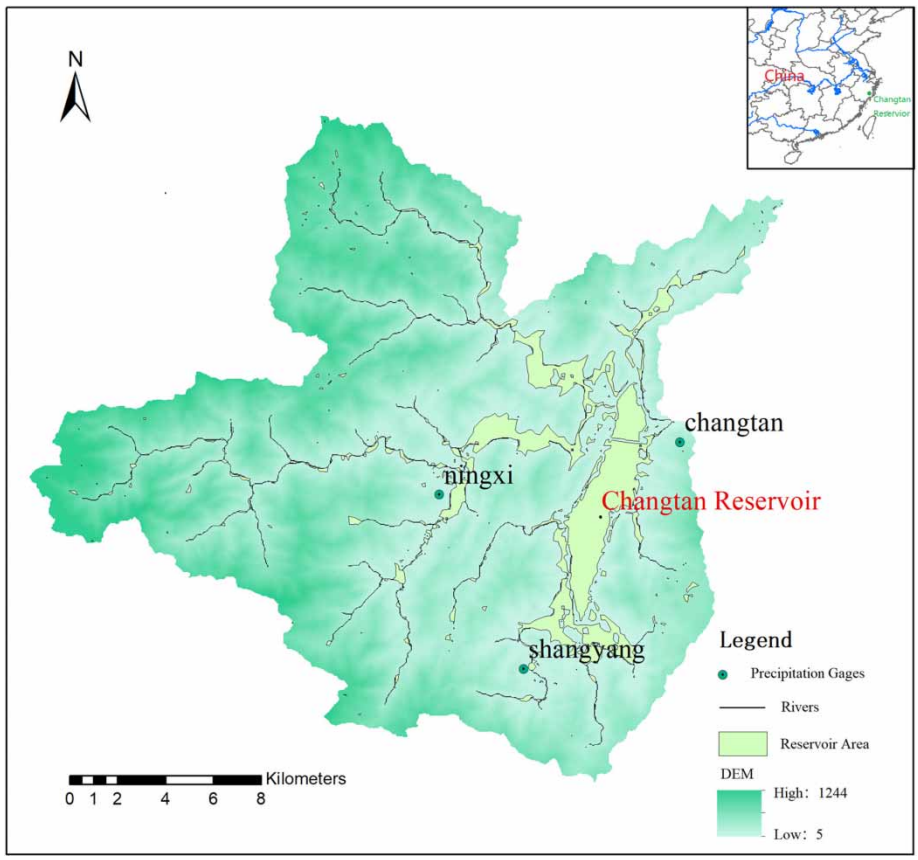

Figure 1 | Changtan Reservior Basin (CRB) and selected precipitation gages.

September, which brings abundant moisture from tropical oceans. Precipitation during these two rainy seasons accounts for 75–85% of total annual precipitation and the storm events during both periods could lead to floods in this region. As a result, the study area faces a great risk of flooding, and the operation of reservoirs requires a better knowledge of precipitation variability and flood forecasting. This issue becomes more critical as the study area is undergoing rapidly changing social dynamics.

Storm properties are analyzed and compared in MFS and TFS using hourly station data. In this study, the MFS ranges from April 16th to July 15th and the TFS ranges from 16 July to 15 October. In this case, the length of MFS and TFS are identical so that the storm properties are comparable. Two stations (ningxi and changtan) were chosen in CRB (Figure 1) with sufficient coverage for a long period (1960–2019) and high-quality data (less than 1% accumulated precipitation data). The Shangyang station is not involved due to the high percentage of missing data. The accumulated data are equally distributed to each hour for the accumulation period (generally 3–8 h) as the calculation of storm properties requires continuous hourly data. The reconstruction will not change the calculation of storm duration, inter-storm period, and average storm intensity based on the definition of these storm properties. It only impacts the determination of the within-storm pattern. However, the accumulated data accounts for less than 1% of the total precipitation data and the calculation of within-storm pattern is conducted on multiple months for a long period. As a result, the reconstruction will have little impact on the determination of storm properties. The future changes in storm properties are determined using hourly precipitation projections from CMIP6 climate models (Eyring *et al.* 2016).

2.2. Analysis on storm properties

The independent storm event is identified from precipitation time series based on a criterion of a specific minimum dry period. The selection of the criterion is arbitrary due to different research purposes. The minimum dry period is set to 6 h in this study, which is corresponding to the average flow concentration time of CRB. An independent storm event could be identified if it separated from the preceding and succeeding precipitation by the minimum dry period or longer. The storm duration, inter-storm period, average storm intensity, and the within-storm pattern could be calculated once a single storm event is identified. Then, the average storm duration (inter-storm period) could be determined by total duration (inter-storm period) divided by the number of storm events (inter-storm periods), and the average storm intensity could be calculated by total precipitation divided by the total duration of the selected storm events, and the within-storm pattern could be characterized using cumulative normalized mass curves (Equation 4 in Figure 2). Storm properties during a certain period, for example, the MFS and TFS, are statistically analyzed from the observed station data and CMIP6 precipitation projections (Figure 2). The differences between each storm property are analyzed for storm events of different magnitudes. To further assess the potential changes in the future, we divided the whole CMIP6 simulation period into three parts: hist (1981–2010), future1 (2021–2050), and future2 (2061–2090). The percentage changes in storm properties were computed by comparing the results from future runs with those from historical runs. The significance of the changes is tested using a permutation resampling method (Yu *et al.* 2015). Sets of years (30 years) are randomly sampled without replacement from both the historical and future periods. Monthly storm properties are calculated for each set of years. The sampling is repeated for 1,000 times and 1,000 sets of storm properties are obtained. Then it is considered significant at the 0.1 level if the magnitude of the storm properties exceeds the 95th or 5th percentile of that determined from the random permutations. We also evaluate the uncertainty of storm properties during the two rainy seasons under four climate change scenarios (Table 1) through the combination of shared socioeconomic pathways (SSPs) and representative concentration pathways (RCPs).

3. RESULTS AND DISCUSSIONS

3.1. Storm properties in MFS and TFS

The maximum monthly storm duration appears in June (Figure 3) during which the precipitation is mainly dominated by the Meiyu system. The relatively longer storm duration is mainly a product of the quasi-stationary front. There are no storm events during this period which has a total amount of precipitation over 250 mm. However, it is worth noting that large storm events with higher average storm intensity also exits during MFS (26 storm event with total precipitation larger than 100 mm, Table 2) due to the quasi-stationary and slow-moving linear mesoscale convective systems (Wang *et al.* 2014). Storms in July and August are characterized by shorter duration and higher intensity as the storms during the hot summer are mainly produced by the local convective systems and typhoons. So, the total precipitation during TFS is larger than that of MFS in the study area while the average account of storm events and the average storm duration are all smaller. In

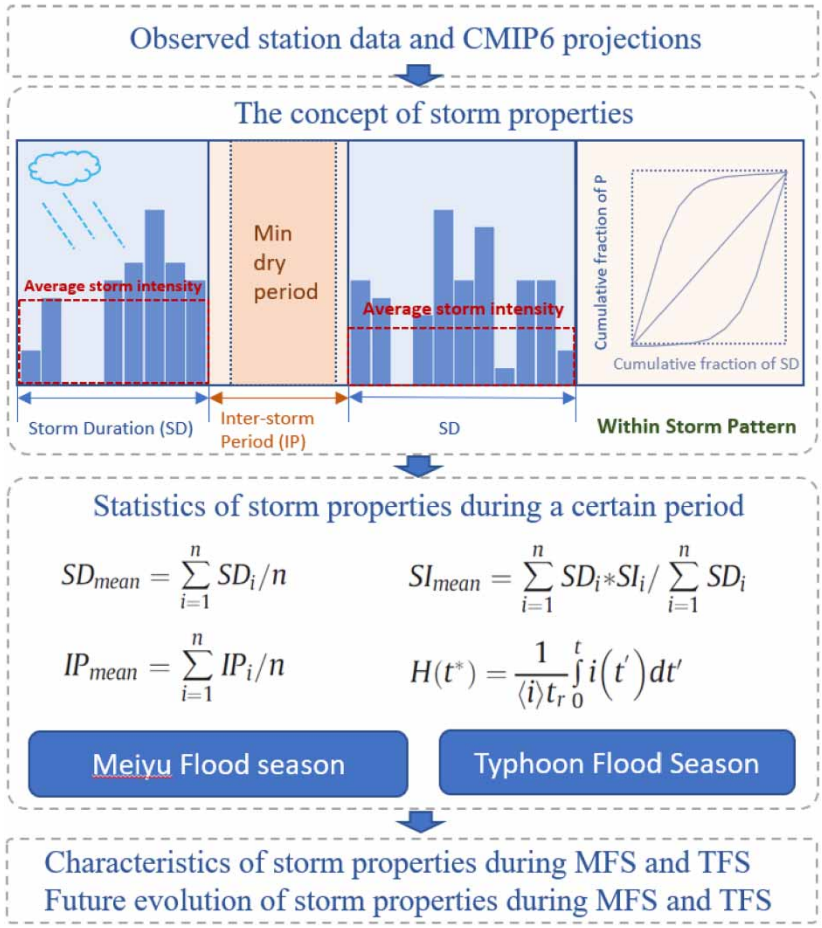

Figure 2 | Conceptual frame work of this study.

Table 1 | New scenarios developed by CMIP6 (O'Neill *et al.* 2016)

	Shared socioeconomic pathways[a]				
2100 forcing level (W/m^2)	**SSP1**	**SSP2**	**SSP3**	**SSP4**	**SSP5**
8.5					SSP585
6.0					
7.0			SSP370		
4.5		SSP245			
3.4					
2.6	SSP126				
1.9					

[a]Five narratives (socioeconomic pathways, SSP scenarios) describing different development paths of society. (SSP1: sustainability, SSP2: middle of the road, SSP3: regional rivalry, SSP4: inequality, and SSP5: fossil fueled development).

other words, the larger precipitation amount during TFS is mainly due to higher intensity storm events, which could be further proved by the account of storm events of which the total precipitation is larger than 250 mm in Table 2. Mass curves of three levels from TFS storm events show a broader range than that of MFS, indicating that the within-storm pattern is more uncertain and unsteady during TFS under the impact of tropical cyclones with huge power and abundant moisture.

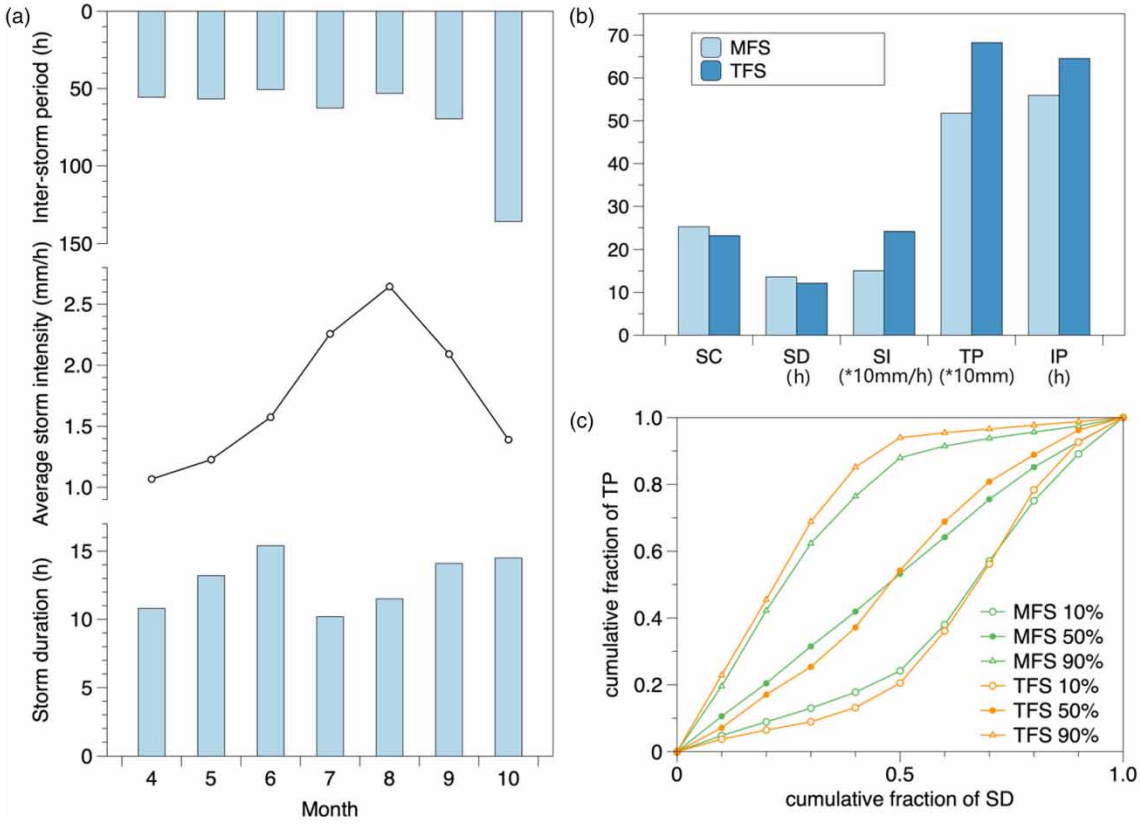

Figure 3 | Storm properties in MFS and TFS ((a) monthly storm duration, inter-storm period, and average storm intensity; (b) storm count, storm duration, storm intensity, total storm precipitation, and inter-storm period in MFS and TFS; (c) mass curves for MFS and TFS).

Table 2 | New scenarios developed by CMIP6 (O'Neill *et al.* 2016)

	MFS				TFS			
TP level (mm)	**SC**	**SD (h)**	**SI (mm/h)**	**TP (mm)**	**SC**	**SD (h)**	**SI (mm/h)**	**TP (mm)**
<10	15.3	6.8	0.635	65.6	12.6	5.6	0.780	55.3
[10,25)	7.7	12.3	1.339	126.5	6.8	9.7	1.710	112.0
[25,50)	5.0	18.4	1.928	177.2	3.7	13.5	2.574	129.2
[50,100)	2.4	27.9	2.433	164.5	2.2	21.9	3.169	149.2
[100,250)	0.4	50.7	2.838	63.4	1.0	46.6	3.295	150.9
≥250	N/A	N/A	N/A	0.0	0.5	65.4	5.125	153.3

3.2. Projected changes of storm properties in MFS and TFS

Previous studies indicate that current climate models tend to simulate longer duration and lower intensity of precipitation than observed due to the 'drizzling problems' in precipitation simulations by most large-scale climate models (Chen *et al.* 1996; Dai 2006; Jiang *et al.* 2013; Mejia *et al.* 2014). This problem is caused by a higher frequency of moisture convection in models than in nature where convective inhibition processes allow atmospheric instability to accumulate before intense convection starts (Dai 2006). However, they can detect the long-term variation and trend of precipitation storm properties impacted by climate change (Jiang *et al.* 2016). Meanwhile, a threshold of '0.1 mm' is used to determine a dry interval to alleviate the impact of 'drizzling' problems. In this study, MIROC6 with a spatial resolution at 1.4° × 1.4° and temporal resolution at 1 h was selected to provide precipitation simulations under different emission scenarios due to its availability in continuous hourly precipitation time series.

The total precipitation, the average storm intensity, and the inter-storm period in MFS during both the future1 and future2 periods show a relatively consistent increasing trend in MFS (Figure 4). However, the increasing total precipitation is caused by different changes in storm properties for different scenarios. The maximum increase of total precipitation (TP) in SSP245 is due to longer storm duration with higher average storm intensity while the frequency of storm events remains steady compared to those determined from historical simulations. The slight increase of TP in SSP126 is accompanied by more frequent storm events with shorter duration and higher average intensity. The results indicate that there are more precipitation extremes during MFS in the future and it will be more obvious during 2061–2090.

In TFS, the maximum increase of TP appears in SSP585 due to a higher average storm intensity, TP exhibits less increase in the other scenarios except for SSP245 for the future1 period. The decrease of TP during this period for SSP245 is accompanied by more moderate storm events with shorter duration. TP in SSP126 also presents an obvious increase during both future periods. However, the increases are caused by changes in different storm properties. During the future1 period, it is mainly due to more high frequency – long duration precipitation events, while during the future2 period, it is mainly induced by storms with higher average intensity. As a whole, the future storm events are characterized by higher average storm intensity and will increase the flood risk in CRB, especially during the SSP585 scenario in the future2 period due to the longer storm duration.

The mass curves determined from historic simulation match well with those determined from future simulations for most emission scenarios at both MFS and TFS (Figure 5), which means that the within storm pattern is relatively stable under future climate change. Some exceptions also exist. For example, the future (both future1 and future2) mass curve range is narrower than the historic mass curve indicating a more stable within storm pattern in the future. This change in the within storm pattern is mainly caused by the changes in 10 percentile curves, which means more intense precipitation at the early age of a storm. Similar changes can be seen in the MFS future1 period for SSP585 and TFS future (both future1 and future2) period for SSP370. On contrast, the mass curve range becomes wider in future2 period than in the historic

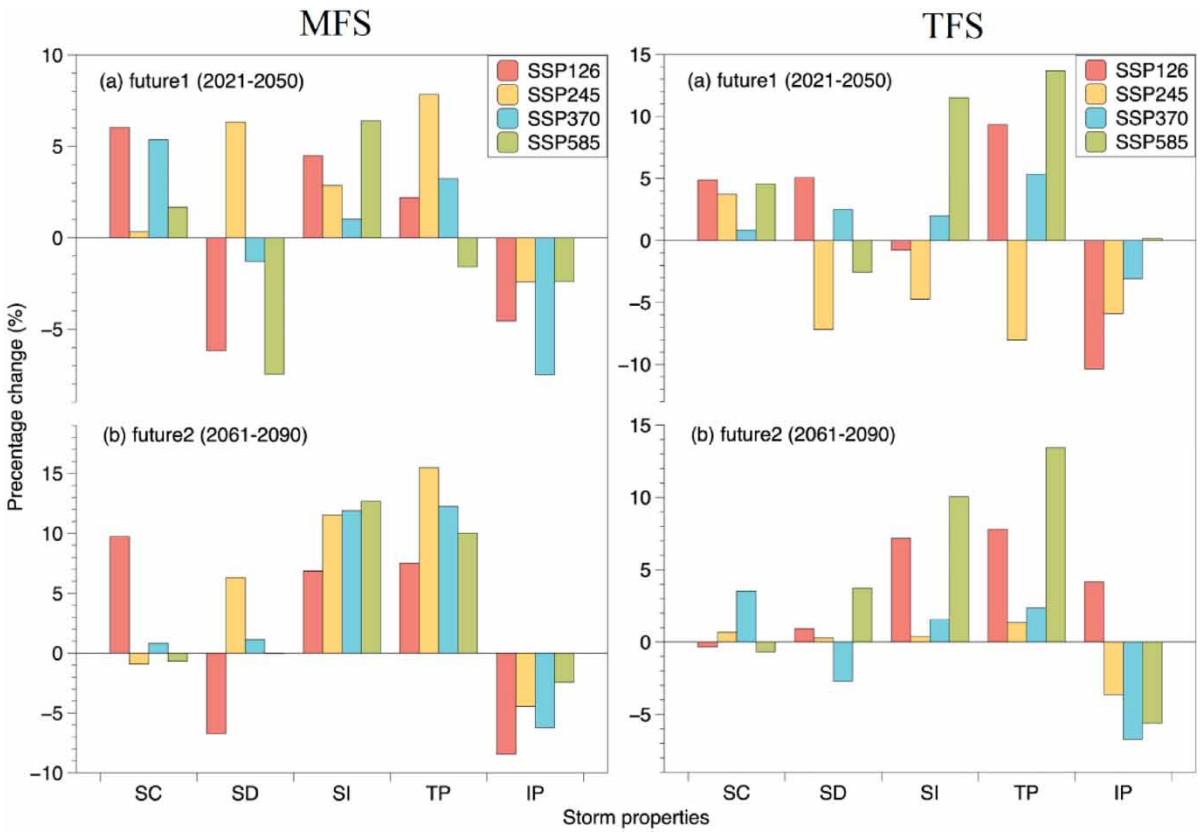

Figure 4 | Future changes ((a) future1; (b) future2) of storm count (SC), storm duration (SD), average storm intensity (SI), total precipitation (TP), and inter-storm period (IP) compared to those of historical period (1981–2010) in MFS (Left) and TFS (Right).

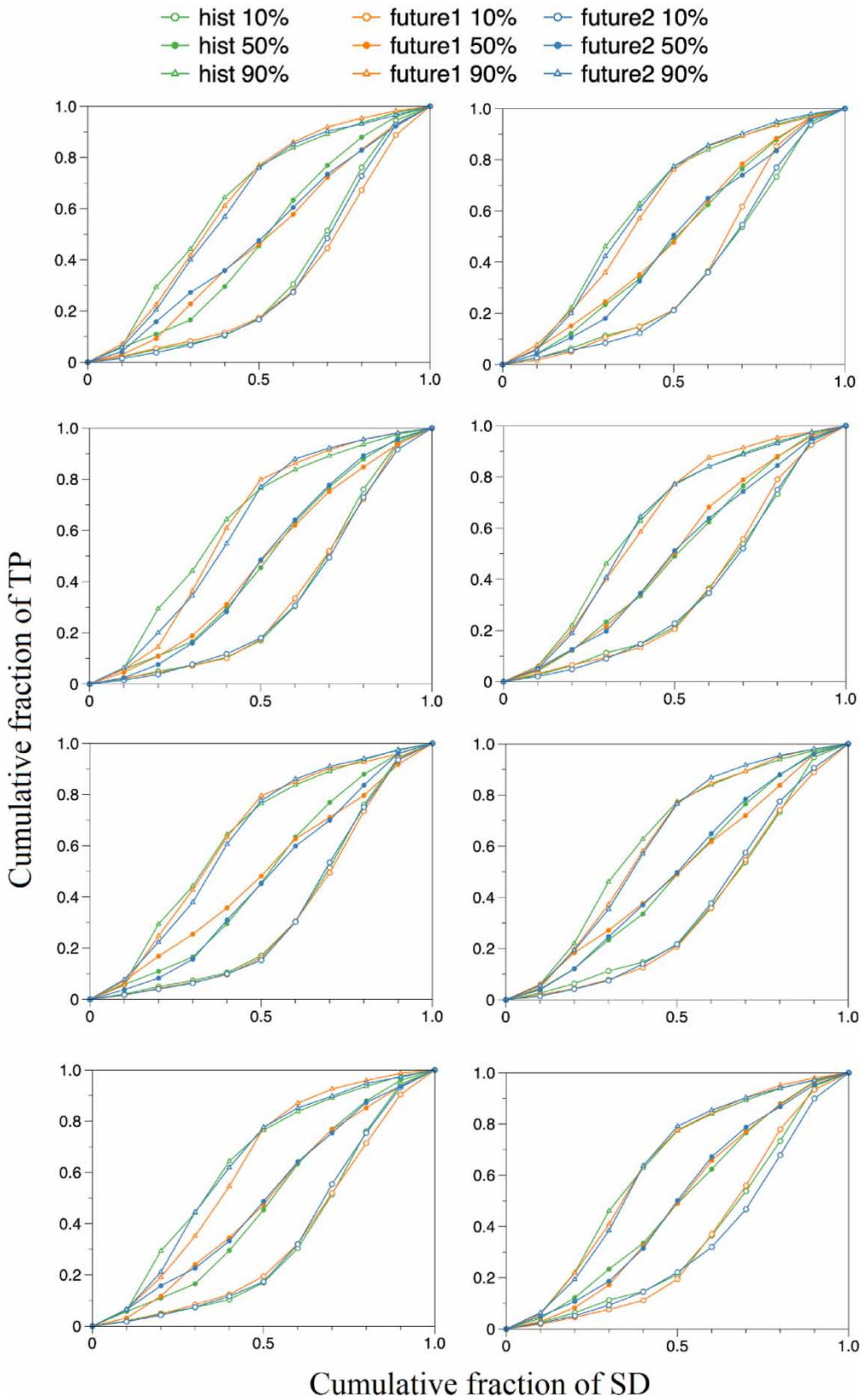

Figure 5 | Mass curves representing within storm pattern in MFS and TFS for different scenarios during historic period, future 1, and future 2.

and future1 period in TFS for SSP585. This is mainly caused by the changes in 90% curves which mean less intense precipitation at the late part of a storm. The within storm pattern becomes more uncertain in TFS for SSP585.

4. DISCUSSIONS AND CONCLUSIONS

In this study, we examine the precipitation characteristics in terms of storm properties in two rainy seasons at CRB. We also investigate the evolution of these storm properties by comparing the statistical matrices from historical and future simulations of selected CMIP6 GCM outputs. Our results highlight the changing patterns of storm duration, inter-storm period, average storm intensity, and within storm pattern in both MFS and TFS, which confirm and extend findings from previous studies (Jiang *et al.* 2016; Guan *et al.* 2020; Chen *et al.* 2022; Wei *et al.* 2022).

Precipitation storms in TFS exhibit shorter duration and higher average storm intensity than those of MFS. In other words, the larger total precipitation in TFS is induced by the higher average intensity of storms under the impacts of the local convective heat transport effects during the hot summers and tropical cyclones. However, this does not mean the risk of floods lies mainly during the TFS. The accumulative precipitation in MFS could also pose a great threat to local reservoirs, especially during June, during which the long-term mean storm duration is the largest of the year.

Future projections of storm properties show uncertainties among different emission scenarios and different seasons. However, the total precipitation and the average storm intensity exhibit a relatively consistently increasing trend while the inter-storm period presents a decreasing trend, especially during MFS. This is probably due to the ability of current GCMs in simulating large-scale frontal systems during MFS rather than local impacts such as local convective heat transport and random impacts on typhoon routine (Vitart *et al.* 1997; Camargo *et al.* 2005; Jiang *et al.* 2013). The uncertainties mainly lie in the projected changes of storm duration, which is not consistent either in magnitude or direction. However, changes in storm durations are not significant compared to changes in the average storm intensity and total precipitation. The higher intensity is the main factor that contributes to the increase in total precipitation during both MFS and TFS. The increase in average storm intensity is accompanied by the increase in storm duration during TFS for SSP585, which may pose the greatest challenges to reservoir operation strategies for mitigating the over level floods. The uncertainty arises not only from the emission scenarios, but also from internal variability and various climatic models (Hawkins & Sutton 2011; Rupp *et al.* 2013; Deser *et al.* 2014). The uncertainty from internal variability is not conducted as the long-term mean storm properties over 30 years which should not be very sensitive to internal variability (Rupp *et al.* 2013). For model uncertainty, there are many precipitation outputs from CMIP6 climate models at monthly and daily temporal scales. However, precipitation projections at an hourly scale are relatively few. Currently, only four hourly precipitation products are available, which may be not enough for a comprehensive evaluation of the uncertainties arising from models. As a result, this study focuses on the uncertainty from different emission scenarios and the model uncertainty could be investigated in future research when more hourly precipitation products are available.

ACKNOWLEDGEMENTS

This work was supported by the Fundamental Research Funds for the Central Universities (Grant No. 2019B05014); the Belt and Road Special Foundation of the State Key Laboratory of Hydrology-Water Resources and Hydraulic Engineering (Grant No. 2020490211; Grant No. 2020490208). We wish to thank the Program for Climate Model Diagnosis & Intercomparison (PCMDI) Earth System Model Evaluation Project for provide the data used in this paper.

DATA AVAILABILITY STATEMENT

All relevant data are available from https://github.com/pengjiang-hhu/HYDROLOGY-D-22-00142

CONFLICT OF INTEREST

The authors declare there is no conflict.

REFERENCES

Agilan, V. & Umamahesh, N. 2016 Is the covariate based non-stationary rainfall IDF curve capable of encompassing future rainfall changes? *Journal of Hydrology* **541**, 1441–1455.

Angel, J. R., Palecki, M. A. & Hollinger, S. E. 2005 Storm precipitation in the United States. Part II: soil erosion characteristics. *Journal of Applied Meteorology* **44** (6), 947–959.

Camargo, S. J., Barnston, A. G. & Zebiak, S. E. 2005 A statistical assessment of tropical cyclone activity in atmospheric general circulation models. *Tellus A: Dynamic Meteorology and Oceanography* **57** (4), 589–604.

Chen, M., Dickinson, R. E., Zeng, X. & Hahmann, A. N. 1996 Comparison of precipitation observed over the continental United States to that simulated by a climate model. *Journal of Climate* **9** (9), 2233–2249.

Chen, J., Brissette, F. P., Chaumont, D. & Braun, M. 2013 Finding appropriate bias correction methods in downscaling precipitation for hydrologic impact studies over North America. *Water Resources Research* **49** (7), 4187–4205.

Chen, C.-A., Hsu, H.-H., Liang, H.-C., Chiu, P.-G. & Tu, C.-Y. 2022 Future change in extreme precipitation in East Asian spring and Mei-yu seasons in two high-resolution AGCMs. *Weather and Climate Extremes* **35**, 100408.

Dai, A. 2006 Precipitation characteristics in eighteen coupled climate models. *Journal of Climate* **19** (18), 4605–4630.

Deser, C., Phillips, A. S., Alexander, M. A. & Smoliak, B. V. 2014 Projecting North American climate over the next 50 years: uncertainty due to internal variability. *Journal of Climate* **27** (6), 2271–2296.

Ding, Y., Liu, J., Sun, Y., Liu, Y., He, J. & Song, Y. 2007 A study of the synoptic-climatology of the Meiyu system in East Asia. *Chinese Journal of Atmospheric Sciences-Chinese Edition* **31** (6), 1082.

Eyring, V., Bony, S., Meehl, G. A., Senior, C. A., Stevens, B., Stouffer, R. J. & Taylor, K. E. 2016 Overview of the coupled model intercomparison project phase 6 (CMIP6) experimental design and organization. *Geoscientific Model Development* **9** (5), 1937–1958.

Gao, L., Huang, J., Chen, X., Chen, Y. & Liu, M. 2017 Risk of extreme precipitation under nonstationarity conditions during the second flood season in the Southeastern Coastal Region of China. *Journal of Hydrometeorology* **18** (3), 669–681. doi:10.1175/JHM-D-16-0119.1.

Guan, P., Chen, G., Zeng, W. & Liu, Q. 2020 Corridors of Mei-Yu-season rainfall over eastern China. *Journal of Climate* **33** (7), 2603–2626.

Hawkins, E. & Sutton, R. 2011 The potential to narrow uncertainty in projections of regional precipitation change. *Climate Dynamics* **37** (1–2), 407–418.

Jiang, P., Gautam, M. R., Zhu, J. & Yu, Z. 2013 How well do the GCMs/RCMs capture the multi-scale temporal variability of precipitation in the Southwestern United States? *Journal of Hydrology* **479**, 75–85.

Jiang, Z., Li, W., Xu, J. & Li, L. 2015 Extreme precipitation indices over China in CMIP5 models. Part I: model evaluation. *Journal of Climate* **28** (21), 8603–8619. doi:10.1175/JCLI-D-15-0099.1.

Jiang, P., Yu, Z., Gautam, M. R., Yuan, F. & Acharya, K. 2016 Changes of storm properties in the United States: observations and multimodel ensemble projections. *Global and Planetary Change* **142**, 41–52.

Lima, C. H., Kwon, H.-H. & Kim, J.-Y. 2016 A Bayesian beta distribution model for estimating rainfall IDF curves in a changing climate. *Journal of Hydrology* **540**, 744–756.

Liu, L., Wang, X., Feng, G., Dogar, M. M., Zhang, F., Zhiqiang, G. & Zhou, B. 2021 Variation of main rainy-season precipitation in eastern China and relevance to regional warming. *International Journal of Climatology* **41** (3), 1767–1783.

Liuzzo, L., Notaro, V. & Freni, G. 2017 Uncertainty related to climate change in the assessment of the DDF curve parameters. *Environmental Modelling & Software* **96**, 1–13. doi:10.1016/j.envsoft.2017.06.044.

Mejia, J. F., Niswonger, R. G. & Huntington, J. 2014 *Uncertainty Transfer in Modeling Layers: From GCM to Downscaling to Hydrologic Surface-Groundwater Modeling.*

Niu, Z., Feng, L., Chen, X. & Yi, X. 2021 Evaluation and future projection of extreme climate events in the Yellow River basin and Yangtze river basin in China using ensembled CMIP5 models data. *International Journal of Environmental Research and Public Health* **18** (11), 6029.

O'Neill, B., Tebaldi, C., Van Vuuren, D, Eyring, V., Friedlingstein, P., Hurtt, G., Knutti, R., Kriegler, E., Lamarque, J. & Lowe, J. 2016 The scenario model intercomparison project (ScenarioMIP) for CMIP6. *Geoscientific Model Development* **9** (9), 3461–3482.

Pathirana, A., Denekew, H. B., Veerbeek, W., Zevenbergen, C. & Banda, A. T. 2014 Impact of urban growth-driven landuse change on microclimate and extreme precipitation – a sensitivity study. *Atmospheric Research* **138**, 59–72.

Qiao, S., Chen, D., Wang, B., Cheung, H. N., Liu, F., Cheng, J., Tang, S., Zhang, Z., Feng, G. & Dong, W. 2021 The longest 2020 Meiyu season over the past 60 years: subseasonal perspective and its predictions. *Geophysical Research Letters* **48** (9), e2021GL093596.

Rupp, D. E., Abatzoglou, J. T., Hegewisch, K. C. & Mote, P. W. 2013 Evaluation of CMIP5 20th century climate simulations for the Pacific Northwest USA. *Journal of Geophysical Research: Atmospheres* **118** (19), 10,884–810,906.

Sohoulande Djebou, D. C. & Singh, V. P. 2016 Impact of climate change on precipitation patterns: a comparative approach. *International Journal of Climatology* **36** (10), 3588–3606.

Tian, Y., Xu, Y.-P., Booij, M. J., Lin, S., Zhang, Q. & Lou, Z. 2012 Detection of trends in precipitation extremes in Zhejiang, east China. *Theoretical and Applied Climatology* **107** (1), 201–210.

Trenberth, K. E. 2011 Changes in precipitation with climate change. *Climate Research* **47** (1–2), 123–138.

Vitart, F., Anderson, J. & Stern, W. 1997 Simulation of interannual variability of tropical storm frequency in an ensemble of GCM integrations. *Journal of Climate* **10** (4), 745–760.

Volonté, A., Muetzelfeldt, M., Schiemann, R., Turner, A. G. & Klingaman, N. 2021 Magnitude, scale, and dynamics of the 2020 Mei-yu rains and floods over China. *Advances in Atmospheric Sciences* **38** (12), 2082–2096.

Walther, G., Post, E., Convey, P., Menzel, A., Parmesan, C., Beebee, T., Fromentin, J., Hoegh-Guldberg, O. & Bairlein, F. 2002 Ecological responses to recent climate change. *Nature* **416** (6879), 389–395.

Wang, L. & Chen, W. 2014 A CMIP5 multimodel projection of future temperature, precipitation, and climatological drought in China. *International Journal of Climatology* **34** (6), 2059–2078. doi:10.1002/joc.3822.

Wang, X., Cui, C., Cui, W. & Shi, Y. 2014 Modes of mesoscale convective system organization during Meiyu season over the Yangtze River basin. *Journal of Meteorological Research* **28** (1), 111–126.

Wei, L., Liu, L., Jing, C., Wu, Y., Xin, X., Yang, B., Tang, H., Li, Y., Wang, Y. & Zhang, T. 2022 Simulation and projection of climate extremes in China by a set of statistical downscaled data. *International Journal of Environmental Research and Public Health* **19** (11), 6398.

Yu, Z., Jiang, P., Gautam, M. R., Zhang, Y. & Acharya, K. 2015 Changes of seasonal storm properties in California and Nevada from an ensemble of climate projections. *Journal of Geophysical Research: Atmosphere* **120**, 2676–2688. doi:10.1002/2014JD022414.

Zhang, Q., Sun, P., Singh, V. P. & Chen, X. 2012 Spatial-temporal precipitation changes (1956–2000) and their implications for agriculture in China. *Global and Planetary Change* **82**, 86–95.

First received 23 December 2022; accepted in revised form 26 February 2023. Available online 13 March 2023